Received: March 4, 2023. Revised: April 20, 2023.

INASS

International Journal of
Intelligent Engineering & Systems

http://www.inass.org/

Retinal Vasculature Segmentation Based on Morphology and Pixel Level Classification

Azra Fatima[1*] **E. Kiran Kumar[1]**

[1]*Department of Electronics and Communication Engineering, Koneru Lakshmaiah Education, Vaddeswaram, AP,*
* Corresponding author's Email: azra927@gmail.com

Abstract: Retinal images are found as the major resources for the automatic diagnosis of diabetic retinopathy (DR). However, the advanced stages like proliferative diabetic retinopathy (PDR) cause the branch out of new and thin vessels in the retina. These vessels create a lot of confusion at the diagnosis of DR through retinal mages. Hence, this paper proposes a new blood vessels segmentation mechanism in three stages; they are major blood vessels segmentation, minor blood vessels segmentation and post-processing. In the first stage, the retinal image is enhanced for quality enhancement followed low pass filtering and top-hat transform to segment major blood vessels. In the second stage, the residue image left in the first stage is processed for pixel level classification. At this stage, each pixel is represented with a set of 19 features. Then this feature vector is fed to support vector machine (SVM) for classification. Finally, the resultant images obtained in the first two stages are combined to get the final retinal vessel structure. For simulation, we used two standard retinal image datasets namely STARE and CHASE_DB and the performance is measured through sensitivity, accuracy, specificity, Jaccard Similarity index and Dice similarity index. Simulation results show that the proposed method achieved better segmentation accuracy and it is of approximately 96.85% and 96.66% for STARE and CHASE_DB respectively.

Keywords: Retinal vessels, Diabetic retinopathy, Segmentation, Minor blood vessels, Support vector machine.

1. Introduction

Recently diabetic retinopathy (DR) is found as one of the leading eye related disease which can cause to a permanent vision loss if it was unidentified and untreated. At the initial stages of DR, the patients won't experience the vision impairment due to very less or minor symptoms. However with the progress of DR, it may consequences to a vision loss. Hence there is a need of a regular eye checkup to analyze the status of DR through retinal images [1]. However, due to a rapid rise in the DR patients, the available Limited number of eye specialists cannot cope up with the huge number. According to several clinical reports [2, 3], the approximate number of diabetic retinopathy patients is 126.6 million in the year of 2011 and it is predicted to reach 191 million by the year of 2030. Hence, to control the Rapid rise of DR patients, there is a need of an automatic DR diagnosis is very essential.

In an automatic DR diagnosis system, the retinal image is taken as input and its feature are analyzed in different ways to detect the presence and or status of DR. Retinal images are the major sources for the DR diagnosis as the abnormalities raised due to DR are reflected in the retinal images. For example the advanced stages of DR results in the branch out of new vessels. Further, some other symptoms like variations in the structure of retinal vessels, proliferation of new and abnormal vessels, fatty deposits in retina and swelling in macular are the major indicators of DR which can be analyzed through retinal images [4]. Automated blood vessel segmentation helps in the determination of variations in the blood vessels through vessel tortuosity, vessel width, branching patterns and vessel density. Such analyses can help towards the analysis of patients Hypertension variations in the diameters of the retinal vessels due to the past history of cold feet and hands and flicker responses.

In the past several retinal vessel segmentation methods [5, 6] are proposed based on which the proliferative DR (PDR) analysis was executed. These methods employed to mask the retinal vascular structure to make sure that the blood vessels are mistaken for red lesions those are present due to DR. Moreover, for the analysis and identification of PDR, the vessels structure attributes like width, tortuosity and density are need to be clearly analyzed. Moreover, there is a need of faster and accurate DR screening system to determine abnormalities to DR in eye. There are some approaches like template matching and line detector [7, 8] which attained the segmentation accuracy of 92 % at the cost of huge computational complexity. But, obtaining segmentation accuracy more than 92% along with less competition complexity is a tough task. Moreover, there exist several side effects in retinal images like red lesions (hemorrhages and microaneurysms) and brightly lesions (hard exudates and cotton wool spots), illumination variations and abnormal contrast levels. All these side factors show huge impact on the segmentation accuracy. In the advanced stages of DR, the newly branched out vessels are very thin and they almost resemble the properties of background and red lesions. In such case, there must be an effective differentiation between vessels and background.

To words such aspect, this work executes the vessel segmentation task in two stages; they are major blood vessel segmentation and minor blood vessel segmentation. In the first stage, the major blood vessels which are thick and predominant are segmented while in a second stage, the thin and find vessels are segmented. For the first stage, we employed basic morphology and for second phase we employed pixel based classification through machine learning. The major contributions of this work are outlined as follows;

1. To reduce the segmentation complexity, this work separates the major blood vessel pixels from retinal image and applies classification only on few pixels.
2. To achieve better segmentation accuracy at minor vessels, this work proposes to describe the vessel pixels in an effective manner through a composite feature set.

Rest of the paper is organized as follows; section II to explore the details of literature survey over the blood vessel segmentation methods. The proposed method is described in two stages in the section III and they are major blood vessel segmentation and minor blood vessel segmentation. Section IV explores the details of experimental results and performance analysis of the proposed mechanism over different data sets. Section V provides the concluding remarks of this contribution.

2. Literature survey

In the past several authors have proposed several methods to segment the complete retinal vessel structure from the retinal images. Some others applied basic mathematical morphological operations and some authors focused on the pixel classification etc. Here in this section we outline different retinal vessel segmentation methods.

Dash, S et al. [9] proposed a retinal vessel segmentation strategy based on curvelet transform [12] and jerman filters (JF) [10, 11]. JFs are much advantageous in the determination of vessel bifurcations and edges while curvelet transform ensure its robustness against scale and orientational variations. They employed mean C-thresholding algorithm for segmentation. However, JFs cannot determine the bifurcations at minor vessels which are very thin and invisible.

B. Saha Tchinda et al. [13] Adapted for pixel based classification to segment the blood vessel structure from retinal images. They employed the traditional edge detection filters for feature extraction and artificial neural network (ANN) for classification. ANN classifies each pixel of image into two classes they are vessel pixel and non-vessel pixel. However, only edge features cannot provide sufficient discrimination between vessel and non-vessel classes.

U. Dikkala et al. [14] enhanced the quality of retinal image before processing it for segmentation. They applied mathematical morphology for blood vessel segmentation. As an additional step they also tried to separate the noise components from the green plane of fundus image. Mathematical morphology has least performance at the determination of minor vessels which are the key components of DR.

A. K. Shukla et al. [15] focused on blood vessel segmentation from retinal images and applied local covariance based Eigen map and a new fractional filter. The fractional filter is designed based on the weighted fractional derivative and exponential weight factor. Further the base for the modelling of local covariance matrix is 2^{nd} order moments. 2^{nd} order moments are sensitive to noises unless they are combined with other features at training the classifier.

F. Orujov et al. [16] proposed to segment the blood vessels from fundus image through Mandani type-2 fuzzy logic rules. Initially they process the input retinal image for contrast enhancement and

then process through median filter for noise removal. After preprocessing the image, it is transformed into gradient domain and then applied fuzzy rules to get the vessel structure. Fuzzy rules create convergence problem because the minor vessels are not strictly bounded to specific shape and structure.

Bendlet transform (BT) calculate the directional variations of the vessel pixels in image. R. Kushol et al. [17] employed BT to represent each pixel of retinal image through its directional information and applied an ensemble machine learning algorithm for classification. Next, N. Tamim et al. [18] proposed to represent each pixel is represented with 24 features. Totally five types of filters namely local intensity filter, mathematical morphology, phase congruency, difference of Gaussian and Hessian are used. For classification, they applied a multilayer perceptron neural network (MLPNN). Additionally, they applied a mathematical morphology to optimize the segmentation desserts. However, minor vessels mainly characterized through statistical features which is the main limitation.

Y. Lin et al. [19] proposed an automatic blood vessel segmentation mechanism from fundus image based on Edge detection and deep learning. Under the edge detection, they proposed a new detector called as historically nested edge detector (HNED). At preprocessing, they applied a global smoothness regularization scheme based on conditional random field (CRF). For classification, they employed a deep learning strategy. Ç. Sazak et al. [20] proposed a blood vessel segmentation mechanism based on a new morphological transform called as bowler-hat transform (BHTBHT) which is a multiscale vessel enhancement method that combines number of structuring elements to determine the original structure of blood vessels. Next, [21] applied a special filter to enhance the computer aided diagnosis from retinal images with abnormal contrast levels. These special filters have least effect on the classification of minor vessels.

Z. Yan et al. [22] proposed a three stage segmentation mechanism for vessels segmentation. The first stage segments the thicker and darker vessels and the second stage segment the thin and minor vessels. In the third phase, the results obtained at the two stages are combined to get the complete blood vessel structure. Next, to ensure a better discrimination, they reduced the negative effect incurred due to the larger imbalance between major and minor blood vessels. The third stage refines the non-vessel pixels from vessel pixels and improves the consistency. However, they didn’t apply any pre-processing method which enhances the quality of retinal image and impact the segmentation performance.

J. Dash [23, 24] proposed a recursive and unsupervised mechanism for the segmentation of blood vessels from the fundus image. Initially, they concentrated on the quality enhancement and it was done it through CLAHE and grammar correction. Next, for segmentation they applied thresholding operation in an iterative fashion. Morphological cleaning operation is applied to get the complete vessel structure. Without proper set of features, Thresholding produces more misclassifications at vessels classification.

A. Desiani et al. [25] proposed BVU-Net architecture that combines the advantages of VGG and U-Net for vessels segmentation from retinal images. Even though they used advanced deep learning methods, minor vessels determination is tough because of similar nature with background.

T. J. Jebaseeli et al. [26] used tandem pulse coupled neural network (TPCNN) for retinal vessel segmentation. TPCNN extracts features and fed to deep learning based support vector machine (DLBSVM) for classification. TPCNN works on both intra and inter channel linking of the input neurons. X. Wang et al. [27] propose a retinal vessel segmentation Framework based on a new cascade classification framework. They employed an extremely non-linear mahalanobis distance classifier for classification. However, they didn't define the size of the network and it is purely based on the data used for training.

H. A. Ramos et al. [28] preprocess the retinal image for noise removal through a low pass radius filter (LPRF). Then a 30 feature Gaussian fractional derivative and Gabor filter are used to enhance the segmentation performance. Finally morphology and thresholding are applied to completely segment the vessel structure. D.U.N.Qomariah et al. [29] employed MResUNet for the segmentation of Microaneurysms for DR diagnosis from retinal images. However, the advanced stages of DR can be diagnosed perfectly through minor vessels only. L.C. Rodrigues et al. [30] proposed to segment both retinal vascular network and optic disc based on morphology, Hessian and wavelets. They concentrated on the Tubular characteristics of retinal vessels to determine arteries and veins. LPRF is sensitive to the color artifacts and tabular features are sensitive to random noises. Edge features cannot get explored with Gabor and Gaussian features.

E. Cuevas et al. [31] applied and method called lateral Inhibition to segment the blood vessels from fundus images. Lateral inhibition is a nature-inspired

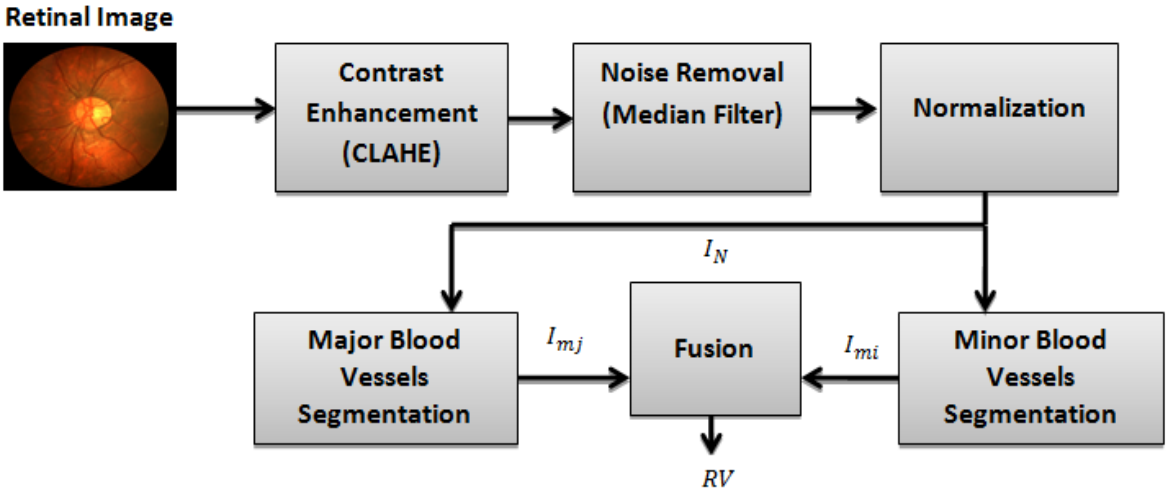

Figure. 1 overall block diagram of proposed vessel segmentation mechanism

Table. 1 List of notations

p	Threshold
I_S^θ	Reconstructed image at angle θ
I_{S_1} & I_{F_1}	Probable major vessels images
I_{mj}	Major blood vessel image
I'_{F_1} & I'_{S_1}	Probable minor vessels images
I_{mi}	Minor vessel image
G_m & G_θ	Gradient magnitude and direction
$E_{i,i\in r,p,s,c,l}$	Edge responses
G_{xx} & G_{yy}	2nd order gradients
SE	Structuring Element

method. In this mechanism, the authors mainly aimed at the improvisation of contrast between background and retinal vessels. Further, they proposed a threshold based on Differential Evaluation and cross entropy to determine whether the pixel belongs to vessel or non-vessel. M.A.U. Khan et al. [32] propose a retinal vessel segmentation mechanism from colour retinal images through an edge detector. Here, the name of the edge detector is mentioned as 2nd order Gaussian derivative kernel. Further, principal component analysis (PCA) is applied as a preprocessing method on the retinal images. Nature inspired methods introduce additional complexity ate the segmentation based classification because more umber of parameters is need o tuned.

B. Toptas and D. Hanbay [41] proposed an 18-F feature vector to represent each pixel in retinal image used ANN for classification. However, they were not able to discriminate the minor vessels from background because; the metrics used by them won't explore the characteristics of minor vessels

In summary, the major problem found from literature survey is very few methods have concentrated on the minor vessels classification. However, they didn't provide a perfect and discriminate feature for describing minor vessels. Hence, the training system get only limited knowledge and misclassifies the minor vessels as background.

3. Proposed framework

3.1 Overview

The proposed method is a novel and efficient vessel segmentation mechanism with segments the entire retinal vessel structure from retinal images. This mechanism segments the entire vessel structure in three stages. In the first stage, it extracts major blood vessels through filtering and Top-Hat transform (THT). Next the second stage focuses on the minor vessels and extracts them through a pixel level classification mechanism. At this stage, each pixel is represented with a composite set of features and classified through SVM algorithm. Once the major and minor vessels are extracted from retinal image individually, they are fused to get a complete retinal vessel structure. Before processing the image for vessel segmentation, it was subjected to pre-processing to enhance the quality. At this stage, we apply the most popular CLAHE algorithm for contrast enhancement. The overall architecture of proposed segmentation mechanism is shown in Fig. 1.

3.2 major blood vessels segmentation

At this stage, the retinal image is processed for Major blood vessel segmentation. Before, the retinal image is processed for quality enhancement. At the time of retinal image requirement, it is acquired at

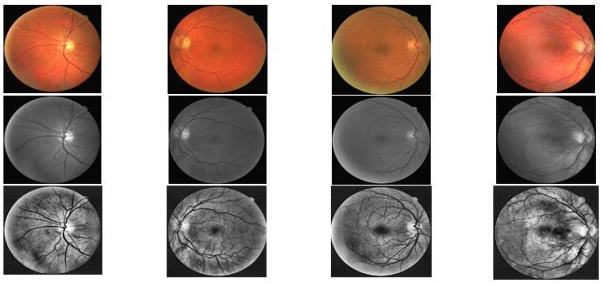

Figure. 2 top row is original color images, second row is green planes and third row is CLAHE outputs

different light intensities which show significant impact on its diagnosis. Hence, we applied the CLAHE algorithm [33] for enhancing the contrast of the retinal image. CLAHE is much beneficial as it enhances the contrast between objects and background of the image. Hence the contrast between background and vessels will get increased. After contrast enhancement, the enhanced image is processed through median filtering for noise removal. A sample of contrast enhanced retinal image is shown in Fig. 2.

Since the vessels are darker the contrast enhanced image elevates them and ensures sufficient discrimination between background and the retinal vessels. Consider *I* be the retinal image and I_C be the contrast enhanced image, then it is subjected to normalisation and each pixel is converted in such a way its pixel intensity lies within the range of 0 and 1.

The normalisation is done by the division of each pixel intensity with the maximum pixel intensity. Consider I_N be the normalised image, it is obtained as $I_N(x,y) = (I_C(\mathrm{x,y}) / \max(I_C))$, where $\max(I_C)$ is the maximum pixel intensity in the contrast enhanced image I_C. Then the normalized image is subjected to extract the major blood vessels segmentation in two phases. In the first phase the normalized image is passed through a Low Pass Filter (LPF) and then subtracted from its original version. Then the resultant image is thresholded against zero and the resultant image is called as high pass filter (HPF) [34] image which consists of the pixels with non-zero pixel intensity. Consider I_F as HPF image, it is obtained as

$$I_F(x,y) = abs(I_N(x,y) - LPF(I_N(x,y))) > 0 \quad (1)$$

Here we apply median filtering for LPF and the size of each window is mentioned as 20*20. Over I_F, we apply the contrast enhancement again to make the retinal vessels more Brighter than background. Next $I_F(x,y)$ is again thresholded against an arbitrary constant p which indicates the threshold of background regions. Due to this thresholding, we are able to extract most of the major vessels. Since our intention is to get complete major blood vessels we fix the p-value to 0.2. An example of major vessel image in first phase is shown in Fig. 3 (b). Consider I_{F_1} be the thresholded HPF image it is obtained as

$$I_{F_1}(x,y) = \begin{cases} 1; & if\, I_F(x,y) > p \\ 0; & otherwise \end{cases} \quad (2)$$

The second phase considers the negative of the normalized image I_N which can be referred as Red regions corresponding to dark pixels in the image. Consider I_R be the resultant image, it is obtained as $I_R = (1 - I_N) \circ g$. Then, I_R is subjected to morphological transform to get different morphological reconstructions. At this phase, we apply THT [35, 36] and derive totally 12 morphological reconstructions. For the derivation of each reconstruction we apply a linear structuring element of length 15 pixels and width 1 pixel. The overall angle considered is 180 degrees and each reconstruction is deviated by an angle of 15 degrees and hence we get totally 12 morphological reconstructions denoted as I_S^θ . Since the retinal vessels are linear and the lengthy structures, we adopted for the linear structuring element. Next, the 12 reconstructions are associated to get a resultant image I_S by considering the maximum value at each pixel. Then I_S is thresholded against *p* to get the final result and let it be denoted as I_{S_1}. An example of major vessel image in second phase is shown in Fig. 3 (c). The following equations explore a simplified process of phase 2;

$$I_S^\theta = THT(I_R), \theta = 0^0 : 15^0 : 180^0 \quad (3)$$

$$I_S(x,y) = \max(I_S^\theta) \quad (4)$$

$$I_{S_1}(x,y) = \begin{cases} 1; & if\, I_S(x,y) > p \\ 0; & otherwise \end{cases} \quad (5)$$

Here I_{S_1} and I_{F_1} are the probable major blood vessel images and they are fused to get the final major blood vessels structure. For this purpose we consider the common pixels in I_{S_1} and I_{F_1} and it is computed as follows

$$I_{mj}(x,y) = \begin{cases} 1; & if\ I_{F_1}(x,y) = 1 = I_{S_1}(x,y) \\ 0; & otherwise \end{cases} \quad (6)$$

Where I_{mj} is the major blood vessel image and an example is shown in Fig. 3 (d).

3.3 Minor blood vessels segmentation

The two resultant images such as I_{H_1} and I_{T_1} obtained in the first phase of the probable major vessel images. Upon the elimination of these two images from the original image, the resultant images are called as probable minor visual images and they are obtained as follows; [34]

$$I'_{F_1} = \begin{cases} 1; & if\ I_{F_1}(x,y) = 1\ and\ I_{mj}(x,y) = 0 \\ 0; & otherwise \end{cases} \quad (7)$$

And

$$I'_{S_1} = \begin{cases} 1; & if\ I_{S_1}(x,y) = 1\ and\ I_{mj}(x,y) = 0 \\ 0; & otherwise \end{cases} \quad (8)$$

Based on the I'_{F_1} and I'_{S_1}, the minor vessel image is derived and is mathematically obtained as

$$I_{mi}(x,y) = \begin{cases} 1; & if\ I'_{F_1}(x,y) = I'_{S_1}(x,y) = 1 \\ 0; & otherwise \end{cases} \quad (9)$$

Then I_{mi} is subjected to pixel-level classification and each pixel in I_{mi} is represented with a composite set of features and classified through SVM algorithm. The details of feature extraction and classification are explored in the following subsections.

3.3.1. Feature extraction

The most important step of pixel-level classification is the determination of features that can help in the accurate classification of minor vessel pixels from the false pixels. Hence, we perform an analysis over different pixel based features those can identify a vessel pixel from its immediate neighbourhood. Further, we choose an optimal set of features which are most suitable for fine vessels segmentation irrespective of variations in FOV, illumination and pathological abnormalities. Here, we refer totally five types of features to describe a pixel in minor vessel image; they are namely edge features, statistical features, morphological features, gradient features and hessian features.

A. Statistical features: Here we extract pixel based statistical features of the minor blood vessel image. These features are very common features and are easily extracted from an image. Here we compute totally 9 features based on the statistical properties of the retinal vessel pixels. For the computation of statistical features, the minor vessel image is processed through windowing and divided it into several Windows by keeping each pixel at the centre of the window. Here we fixed the size of the window as $21 * 21$ [37] and the main reason is that the utilization of 21 pixel structures on retinal images. But the size of Window is variable and it is dependent on the retinal image. The window is slide over the image and we extract totally 9 features from every window. They are namely mean, standard deviation, minimum, maximum, mean absolute deviation (MAD), root sum of squared (RSS) level, skewness, kurtosis and relative neighbourhood discriminator (RND). Mathematically all these features are expressed here;

Mean (μ): it is measured as an average of pixel intensities of all pixels present in a given window $I_{mi}^{w(x,y)}$, where W denotes window and $w(x,y)$ the denotes the centre pixel of window. Consider the pixels present in a window as $(p_1, p_2, \dots, p_k)$ the mean is calculated as

$$\mu = \frac{1}{k}\sum_{n=1}^{k} p_n \quad (10)$$

Standard deviation (σ): standard deviation measures the relative distribution of pixel with respect to mean in a window. Mathematically it is expressed as

$$\sigma = \sqrt{\frac{1}{k}\sum_{n=1}^{k}(p_n - \mu)^2} \quad (11)$$

RSS: it is computed as a square root of aggregated sum of square of pixel intensity is in a window, mathematically it is expressed as

$$RSS = \sqrt{\frac{1}{k}\sum_{n=1}^{k}(p_n)^2} \quad (12)$$

Maximum and Minimum: For a given window with *n* pixels, the maximum feature is identified as the maximum pixel intensity and it is calculated as

$$mx = \max(p_1, p_2, \dots, p_k) \quad (13)$$

Similarly, the minimum feature is identified as the minimum pixel intensity and it is calculated as

$$mn = \min(p_1, p_2, \dots, p_k) \quad (14)$$

MAD: it is measured as an average distance between pixels in a window. It explores the piece of information about variability of pixels in a window. It is computed as

$$MAD = \frac{\sum_i (p_i - \mu)}{n} \quad (15)$$

Kurtosis: kurtosis explores the tails of the distribution and it alleviates the maximum possible difference between tails distribution and Tails of normal distribution. It is mathematically expressed as

$$K = \frac{\mu_3}{\sigma^3} \quad (16)$$

Skewness: Skewness explore the asymmetry between Centre pixel and its neighbour pixels in a given window, mathematically it is expressed as

$$S = \frac{\mu_4}{\sigma^4} \quad (17)$$

RND: it is used to discriminate the false edges those were introduced by bright regions such as optic this and exudates. Mathematically it is expressed as

$$m = \#pixels\ in\ I_{mi}^{w(x,y)} > 0.02\ \&\ RND = \frac{m}{n} \quad (18)$$

B. Edge features

Edges are the sudden grey level changes in an image which can explore the information about retinal vessels starting and ending. For a given image, scanning from left to right or top to bottom the presence of retinal vessels are signified through edge features. There are several edge detection filters which have their own significance in the detection of Edge features [38]. Here we consider totally 5 edge detection filters namely Roberts, Prewitt, Sobel, Canny and Laplacian of Gaussian (LoG). We apply all the five filters on the minor vessel image and final its feature is obtained with the maximum response, it is calculated as

$$E(x,y) = \max\left(E_r(x,y), E_p(x,y), E_s(x,y), E_c(x,y), E_l(x,y)\right) \quad (19)$$

Where

$$E_{i,i\in r,p,s,c,l} = I_{mi} * G_{i,i\in r,p,s,c,l} \quad (20)$$

are the at the edge responses of Roberts, Prewitt, Sobel, Canny and LoG and $G_{i,i\in r,p,s,c,l}$ is the Kernel of corresponding edge detection filters are there Expressed as

$$G_{rx} = \begin{bmatrix} 1 & 0 \\ 0 & -1 \end{bmatrix} \; G_{ry} = \begin{bmatrix} 0 & 1 \\ -1 & 0 \end{bmatrix} \quad (21)$$

$$G_{px} = \begin{bmatrix} -1 & 0 & 1 \\ -1 & 0 & 1 \\ -1 & 0 & 1 \end{bmatrix} \; G_{py} = \begin{bmatrix} -1 & -1 & -1 \\ 0 & 0 & 0 \\ 1 & 1 & 1 \end{bmatrix} \quad (22)$$

$$G_{sx} = \begin{bmatrix} -1 & 0 & 1 \\ -2 & 0 & 2 \\ -1 & 0 & 1 \end{bmatrix} \quad G_{py} = \begin{bmatrix} -1 & -2 & -1 \\ 0 & 0 & 0 \\ 1 & 2 & 1 \end{bmatrix} \quad (23)$$

C. Gradient features: Gradient features explore the directional variation of pixel intensity in an image. As the minor vessels have random directions, the gradient features helps in the determination of proper direction of vessel pixels. Gradient is a scalar value and calculated in both horizontal and vertical directions. Based on the obtained values, the gradient vector is calculated which consists of gradient magnitude (G_m) and gradient direction (G_θ). The calculation of G_m and G_θ from the obtained horizontal and vertical gradients is done as follows

$$G_m(x,y) = \sqrt{(G_x(\mathrm{x,y}))^2 + \left(G_y(\mathrm{x,y})\right)^2} \quad (24)$$

$$G_\theta(x,y) = \tan^{-1}\left(\frac{G_y(\mathrm{x,y})}{G_x(\mathrm{x,y})}\right) \quad (25)$$

Where

$$G_x(\mathrm{x,y}) = I_{mi}(x+1,y) - I_{mi}(x-1,y) \quad (26)$$

And

$$G_y(\mathrm{x,y}) = I_{mi}(x,y+1) - I_{mi}(x,y-1) \quad (27)$$

Here we consider totally four features such as G_x, G_y, G_m and G_θ. Under gradient feature set, each pixel is represented with these four features. The gradient magnitude improves the contrast of blood vessels well and gradient direction explores the feature vector in a pixel curve

D. Hessian features: Hessian matrix (HM) is constructed based on the second order derivatives of a pixel. HM captures the structural characteristics of retinal vessel pixels and it is represented as

$$H = \begin{bmatrix} G_{xx} & G_{xy} \\ G_{yx} & G_{yy} \end{bmatrix} \quad (28)$$

Where G_{xx} and G_{yy} are second order gradient along X- and Y directions respectively. G_{xy} is the gradient on Y parameter in X- direction and G_{yx} is a gradient on X parameter in Y-direction. Generally the backgrounds second order gradients are very small which indicate the second order derivatives separate the background structure from blood vessels effectively.

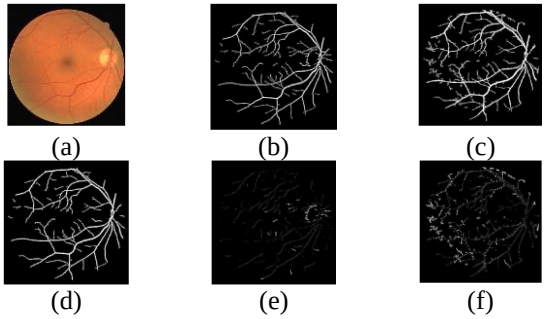

Figure. 3 : (a) Original color retinal image, (b) HPF image (I_{F_1}), (c) THT reconstructed image (I_{S_1}), (d) Major vessel image (I_{mj}) and (d) Minor vessel image (I'_{F_1}) and (f) Minor vessel image (I'_{S_1})

E. Morphological features: Mathematical Morphology (MM) is generally applied to preserve the basic properties of the image. Dilation and Erosion are the two basic MM operations. Dilation followed by erosion is called as opening and erosion followed by dilation is called as closing. Here we used to top-hat and bottom-hat transforms to ensure the clarity of the effect of blood vessels on background. Top hat transform acts like a HPF and hence it extracts brighter regions those or smaller than the mask. Next bottom hat transform shows significant effect on the image background. The mathematical computation of top hat transform and bottom hat transform is done through the following equations

$$THT(I_{mi}) = I_{mi} - (I_{mi} \circ SE) \tag{29}$$

And

$$BHT(I_{mi}) = (I_{mi} \cdot SE) - I_{mi} \tag{30}$$

Where SE is the structuring element, $\circ$ denotes opening operation and $\cdot$ denotes closing operation. Here we employed a linear structuring element of length 15 pixels and width of 1 pixel.

3.3.2. Classification

Once each pixel in minor blood vessel image is represented with all features, then they are fed to SVM algorithm for classification. SVM is a binary classifier which classifies each pixel into two classes they are vessel pixel and non-vessel pixel or background pixel. At SVM algorithm, we employed radial basis function (RBF) kennel.

3.4 Post processing

At this phase, I'_{mi} and I_{mj} are combined to get the complete retinal vessel structure where I'_{mi} is the Minor vessel image after pixel level classification. For complete vascular structure segmentation we applied fusion operation between I'_{mi} and I_{mj} as $RV = I_{mj} \cup I'_{mi}$, where RV denotes the complete retinal vascular structure.

4. Simulation results

In this section, the performance of proposed segmentation mechanism is analyzed by applying it over different types of fundus images. The simulation is done through MATLLAB tool in the personal computer with 1 TB Hard disk and 4 GB RAM. Here, initially, we explore the details of datasets used for simulation. Next, we explore the performance metrics and then the results are followed by comparison.

4.1 Datasets

STARE: This dataset [39] contains totally 397 digitalized eye fundus images. They are acquired with the help of a TopCon TVR-50 Fundus camera with 35^0 FOV. Each image is of the spatial resolution 605×700 pixels. In this dataset, the manually segmented images are available that were segmented by two observers. The first observer segmented 10.4% of the whole image pixels as vessel pixels and the second observer segmented 14.9% pixels as vessel pixels. Two datasets include both the healthy and disease effected images that consist of DR, vascular abnormalities, Choroidal neovascularization, Arteriosclerotic retinopathy, and some others. The segmented results on the accomplishment of proposed mechanism over DRIVE dataset is as shown in Fig. 4.

CHASE_DB: This dataset [40] consists of totally 28 eye fundus image and the resolution of each image is observed as 1280×960. This dataset consists of two sets of manually segmented vascular images with annotations. The first set composed of training images and the second set is of human baseline. The segmented results on the accomplishment of proposed mechanism over DRIVE dataset are shown in Fig. 5.

4.2 Performance metrics

For subjective analysis, we have considered several performance metrics. Firstly, some reference measures like false positive (FP), false negative (FN),

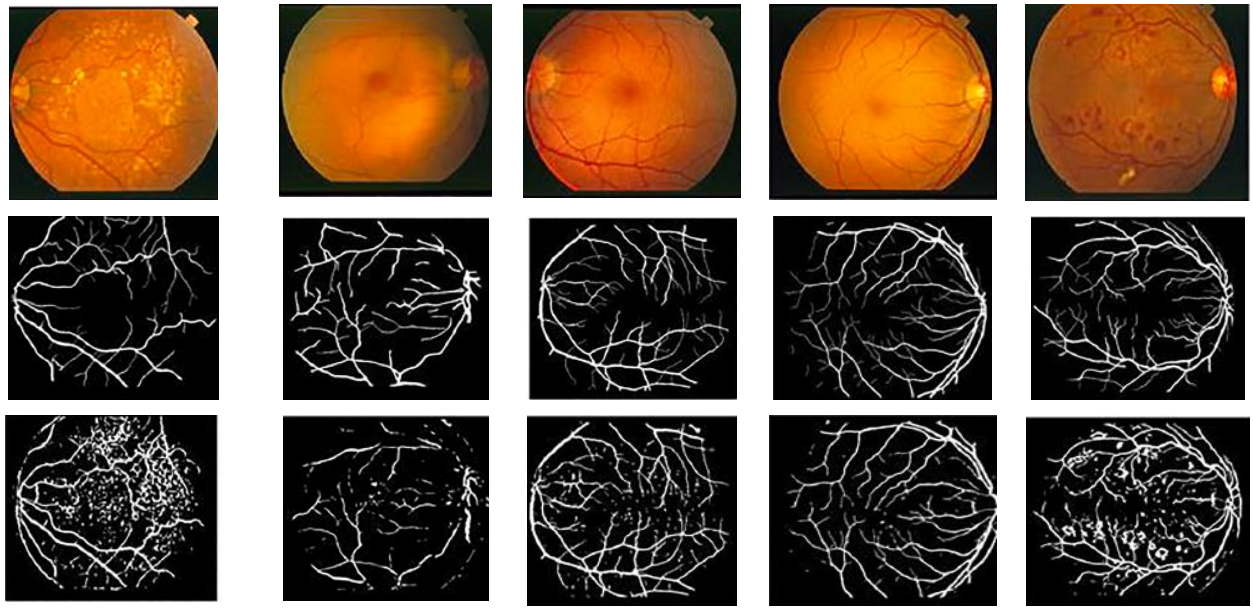

Figure. 4 Results of STARE dataset, First row is original color fundi images, second row are ground truth images and Third row are segmented vasculature through proposed method

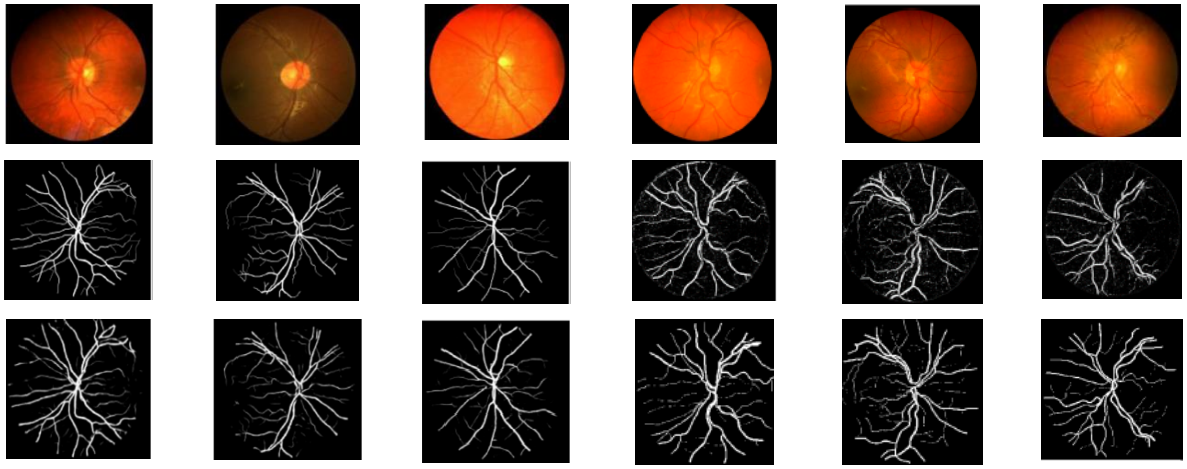

Figure. 5 Results of CHASE_DB dataset, first row is original color fundi images, second row are ground truth images and Third row are segmented vasculature through proposed method

Table.2 Performance metrics for vessel segmentation mechanism

Metric	Formula
Sensitivity	$\frac{TP}{TP+FN}$
Specificity	$\frac{TN}{TN+FP}$
Accuracy	$\frac{TP+TN}{TP+TN+FP+FN}$
Jaccard Similarity Index	$\frac{\lvert A \cap B \rvert}{\lvert A \cup B \rvert}$
Dice Similarity Index	$\frac{2 * \lvert A \cap B \rvert}{\lvert A \rvert + \lvert B \rvert}$

true positive (TP) and true negative (TN) are evaluated based on the obtained segmentation results.

(i) TP: Total number of vessels pixels those classified as vessel pixels.
(ii) TN: Total number of non-vessels pixels those classified as non-vessel pixels.
(iii) FP: Total number of non-vessel pixels those classified as vessel pixels.
(iv) FN: Total number of vessel pixels classified as non-vessel pixels

Based on these secondary metrics, accuracy, specificity (precision), and sensitivity (true positive rate), are shown in Table.1.

The results of the proposed approach on STARE dataset are shown in Table. 3. From the results of Table. 3, we can see that the maximum Sensitivity is observed at 'Im00082.ah' while minimum sensitivity is observed at 'I0003.ah'. The approximate maximum and minimum values are observed as

Table. 3 Performance metrics of proposed method over STARE dataset

Image Sample	Sensitivity	Specificity	Accuracy	Jaccard Index	Dice Index	Time (Sec)
Im0001.ah	0.6416	0.9872	0.9481	0.5355	0.6925	20.2025
Im0002.ah	0.5699	0.9877	0.9452	0.4625	0.6285	20.7774
I0003.ah	**0.3878**	**0.9991**	**0.9082**	**0.3627**	**0.5244**	**21.3625**
I0004.ah	0.8025	0.9685	0.9541	0.4335	0.6001	21.5625
I0005.ah	0.5763	**0.9831**	0.9235	0.4725	0.6402	21.3333
Im00044.ah	0.6285	0.9932	0.9533	0.5352	0.6955	21.4578
Im00077.ah	0.6969	0.9997	0.9585	0.6402	0.7804	21.2365
Im00081.ah	0.7035	0.9963	0.9652	0.6514	0.7874	21.7214
Im00082.ah	**0.8285**	0.9987	**0.9763**	**0.7336**	**0.8475**	21.4752
Im000.39.ah	0.5653	0.9963	0.9355	0.5122	0.6777	**20.7340**

Table. 4 Performance metrics of proposed method over CHASE_DB dataset

Retina Image	Sensitivity	Specificity	Accuracy	Jaccard Index	Dice Index	Time (Sec)
R1	0.6289	0.9797	0.9431	0.5285	0.6810	39.6582
R2	0.5532	0.9778	0.9377	0.4525	0.6165	39.6985
R3	**0.3659**	0.9910	**0.9012**	**0.3515**	**0.5113**	**40.6320**
R4	0.7874	**0.9539**	0.9437	0.4215	0.5879	40.5241
R5	0.5556	0.9742	0.9210	0.4617	0.6268	40.3888
R6	0.6047	0.9893	0.9436	0.5239	0.6873	40.3457
R7	0.6736	0.9980	0.9504	0.6325	0.7638	40.3254
R8	0.6895	**0.9991**	0.9548	0.6454	0.7756	40.6362
R9	**0.8111**	0.9898	**0.9723**	**0.7321**	**0.8395**	40.4512
R10	0.5487	0.9896	0.9663	0.5085	0.6636	**39.7523**

0.8285 and 0.3878 respectively. Next the maximum and minimum specificity are observed at 'I0003.ah', and 'I0005.ah' respectively and the approximate values are 0.9991 and 0.9831 respectively. The maximum accuracy is observed at 'Im00082.ah' while minimum sensitivity is observed at 'I0003.ah' respectively with approximate values of 0.9763 and 0.9082 respectively. For Jaccard Similarity index, the maximum is observed at 'Im00082.ah' and the approximate value is 0.7336. Next, the minimum Jaccard Similarity index is observed at 'I0003.ah' and the approximate value is 0.3627. Finally, the maximum and minimum Dice similarity index are observed at 'I00082.ah', and 'I0003.ah' respectively and the approximate values are 0.8475 and 0.5244 respectively.

The test results of the proposed segmentation mechanism on CHASE_DB1 dataset are shown in Table. 4. From the results of Table. 4, we can see that the maximum Sensitivity is observed at 'R9' while minimum sensitivity is observed at 'R3. The approximate maximum and minimum values are observed as 0.8111 and 0.3659 respectively. Next the maximum and minimum specificity are observed at 'R8, and 'R4 respectively and the approximate values are 0.9991 and 0.9539 respectively. The maximum accuracy is observed at 'R9' while minimum sensitivity is observed at 'R3' respectively with approximate values of 0.9723 and 0.9012 respectively. For Jaccard Similarity index, the maximum is observed at 'R9' and the approximate value is 0.7321. Next, the minimum Jaccard Similarity index is observed at 'R3' and the approximate value is 0.3515. Finally, the maximum and minimum Dice similarity index are observed at 'R9', and 'R3' respectively and the approximate values are 0.8395 and 0.5113 respectively.

Along with recognition assessing performance metrics, we measured the computational time for each image to get segmented by the proposed approach. From the Table. 3 and Table. 4, we can see that the time taken for images of STARE is less than the images of CHAS_DB. The main reason is that the size of images of STARE is less than the size of images of CHASE_DB, as they are 605×700 and 1280×960 respectively. Hence the time of CHASE_DB is approximately double the time of STARE.

Table. 5 explores the effectiveness of proposed vessel segmentation mechanism by comparing its performance with existing methods. Towards the comparison, we referred the methods those have used the same datasets for experimental validation. From the comparison, it can be noticed that the proposed approach has outperformed all the existing methods, as it processes the retinal image in two stages. The methods in [13, 18, 41] and [22] applied the strategy of pixel based classification directly on the quality enhanced retinal image. They got superior performance in the segmentation of major blood

Table. 5 performance comparison between proposed and existing methods

Author	Dataset	Accuracy	Specificity	Sensitivity	Year
Yan et al. [22]	STARE	0.9638	0.9857	0.7735	2019
Sazak et al. [20]	STARE	0.9620	0.9790	0.7300	2019
Tehinda et al [13]	CHASE_DB	0.9452	0.9658	0.7279	2021
	STARE	0.9456	0.9759	0.7265	
Shukla et al [15]	STARE	0.9573	0.9863	0.7023	2020
Orujov et al. [16]	STARE	0.8650	0.8806	0.8342	2020
Kushol et al. [17]	STARE	0.9528	0.9746	0.7798	2020
Tamim et al. [18]	STARE	0.9632	0.9825	0.7806	2020
Lin et al. [19]	CHASE_DB	0.9587	-	0.7815	2019
Khan et al. [21]	STARE	0.9513	0.9812	0.7521	2019
Buket Toptas [41]	STARE	0.9456	0.9824	0.6308	2021
Proposed	STARE	**0.9685**	**0.9869**	**0.8564**	-NA-
	CHASE_DB	**0.9666**	**0.9812**	**0.8114**	

vessels as they look much brighter at the contrast enhancement. However, they were not able to discriminate the minor vessels from background because; the metrics used by them won't explore the characteristics of minor vessels. For the retinal images with advanced stage of DR like PDR, these methods have limited performance due to the presence of newly branched out minor vessels. The newly emerged vessels are in resemblance with background and they can't be classified perfectly. Some methods like [15] and [17] applied transformation and filtering techniques to segment the vessels structure. However, they had shown limited performance than the pixel based classification methods. The remaining methods such as morphological transform [20], edge detector [19], and unsupervised fuzzy learning [16] are also had shown limited segmentation compared to the proposed method. As the alone morphology or filtering or edge detection cannot support for an accurate vessels segmentation because the retinal images are composed of so many attributes along with external effects. In summary, we can say that the proposed mechanism can segment almost entire retinal vessel structure from any kinds of images.

5. Conclusion

Blood vessels are one of the significant attributes of retinal image through which the diagnosis of DR is carried out. For this purpose, they need to be segmented and analyzed. Towards such prospect, this paper proposed a simple and effective blood vessel segmentation mechanism based on the morphology and pixel based classification. The major feature of this approach is to separate the thick and major blood vessels from minor and thin vessels. For the segmentation of major blood vessels, we applied simple morphology and high pass filtering because, the vessels reflects the edge properties in retinal image. For minor vessels segmentation, we applied pixel level classification strategy in which each pixel is described through a set of features based on five different filters. For classification, we applied SVM algorithm which classifies each pixel into two classes; they are vessel and on-vessel. As the number of pixels are reduced from retinal images, then the pixel based classification can be applied only on few pixels and reduces the computational time. Moreover, the composite features explore the better discrimination between vessels and background and helps in the improvisation of segmentation accuracy. Simulation on STARE and CHASE_DB proves the outstanding performance of proposed approach. On an average, the proposed method gained an improvement of 2.29% in accuracy 0.45% in specificity and 22.56% from recent method.

Conflicts of interest

The authors declare no conflict of interest.

Author contributions

Conceptualization, Design, Development and implementation of proposed vessel segmentation by Azra Fatima and Validation and proofread by Kiran Kumar.

References

[1] L. Xu, Y. Wang, Y. Li, Y. Wang, T. Cui, J. Li, and J. B. Jonas, "Causes of blindness and visual impairment in urban and rural areas in Beijing: the Beijing eye study", *Ophthalmology*, Vol. 113, No. 7, pp. 1134–e1, 2006.

[2] N. Congdon, Y. Zheng, and M. He, "The worldwide epidemic of diabetic retinopathy", *Indian J. Ophthalmology*, Vol. 60, No. 5, pp. 428-431, 2012.

[3] J. W. Y. Yau, S. L. Rogers, R. Kawasaki, E. L. Lamoureux, J. W. Kowalski, T. Bek, S. J. Chen, J. M. Dekker, A. Fletcher, J. Grauslund, S. Haffner, R. F. Hamman, M. K. Ikram, T. Kayama, B. E. K. Klein, R. Klein, S. Krishnaiah, K. Mayurasakorn, J. P. O'Hare, T. J. Orchard, M. Porta, M. Rema, M. S. Roy, T. Sharma, J. Shaw, H. Taylor, J. M. Tielsch, R. Varma, J. J. Wang, N. Wang, S. West, L. Xu, M. Yasuda, X. Zhang, P. Mitchell, and T. Y. Wong, "Global prevalence and major risk factors of diabetic retinopathy", *Diab. Care*, Vol. 35, No. 3, pp. 556–564, 2012.

[4] S. D. Candrilli, K. L. Davis, H. J. Kan, M. A. Lucero, and M. D. Rousculp, "Prevalence and the associated burden of illness of symptoms of diabetic peripheral neuropathy and diabetic retinopathy", *J. Diab. Comp*., Vol. 21, No. 5, pp. 306–314, 2007.

[5] S. R. Chowdhury, D. D. Koozekanani, and K. K. Parhi, "Screening fundus images for diabetic retinopathy", In: *Proc., of Forty Sixth Asilomar Conference on Signals, Systems and Computers (ASILOMAR)*, CA, USA, pp. 1641–1645, 2012.

[6] S. R. Chowdhury, D. Koozekanani, and K. Parhi, "Dream: Diabetic retinopathy analysis using machine learning", *IEEE Journal of Biomedical and Health Informatics*, Vol. 18, No. 5, pp. 1717-1728, 2013.

[7] R. Perfetti, E. Ricci, D. Casali, and G. Costantini, "Cellular neural networks with virtual template expansion for retinal vessel segmentation", *IEEE Transactions on Circuits and Systems II: Express Briefs*, Vol. 54, No. 2, pp. 141–145, 2007.

[8] G. Kovács and A. Hajdu, "A self-calibrating approach for the segmentation of retinal vessels by template matching and contour reconstruction", *Med Image Anal*., Vol. 29, pp. 24-46, 2016.

[9] S. Dash, S. Verma, Kavita, M. S. Khan, M. Wozniak, J. Shafi, M. F. Ijaz, "A Hybrid Method to Enhance Thick and Thin Vessels for Blood Vessel Segmentation", *Diagnostics*, Vol. 11, No. 11, p. 2017, 2021.

[10] T. Jerman, F. Pernu, B. Likar, and Z. Špiclin, "Beyond Frangi: An improved multiscale vesselness filter", *Medical Imaging: Image Processing*, Vol. 9413, 2015.

[11] T. Jerman, F. Pernuš, B. Likar, Z. Špiclin, "Enhancement of vascular structures in 3D and 2D angiographic images", *IEEE Trans. Med. Imaging*, Vol. 35, pp. 2107–2118, 2016.

[12] S. S. Kar and S. P Maity, "Blood vessel extraction and optic disc removal using curvelet transform and kernel fuzzy c-means", *Comput. Biol. Med*., Vol. 70, pp. 174–189, 2016.

[13] B. S. Tchinda, D. Tchiotsop, M. Noubom, V. L. Dorr, and D. Wolf, "Retinal blood vessels segmentation using classical edge detection filters and the neural network", *Informatics Med. Unlocked*., Vol. 23, p. 100521, 2021.

[14] U. Dikkala, P. Jaya, C. Engineering, and P. Jaya, "A comprehensive analysis of morphological process dependent retinal blood vessel segmentation", In: *Proc., of International Conference on Computing, Communication, and Intelligent Systems (ICCCIS)*, Noida, India, pp. 510–516, 2021.

[15] A. K. Shukla, R. K. Pandey, and R. B. Pachori, "A fractional filter based efficient algorithm for retinal blood vessel segmentation", *Biomed. Signal Process., Control*., Vol. 59, p. 101883, 2020.

[16] F. Orujov, R. Maskeliunas, R. Damaˇseviˇcius, and W. Wei, "Fuzzy based image edge detection algorithm for blood vessel detection in retinal images", *Appl. Soft Comput. J.*, Vol. 94, p. 106452, 2020.

[17] R. Kushol, M. H. Kabir, M. A. A. Wadud, and M. S. Islam, "Retinal blood vessel segmentation from fundus image using an efficient multiscale directional representation technique Bendlets", *Math., Biosci., Eng*., Vol. 17, pp. 7751–7771, 2020.

[18] N. Tamim, M. Elshrkawey, G. A. Azim, and H. Nassar, "Retinal blood vessel segmentation using hybrid features and multi-layer perceptron neural networks", *Symmetry (Basel)*., Vol. 12, No. 6, pp. 894-899, 2020.

[19] Y. Lin, H. Zhang, and G. Hu, "Automatic Retinal Vessel Segmentation via Deeply Supervised and Smoothly Regularized Network", *IEEE Access*, Vol. 7, pp. 57717–57724, 2019.

[20] Ç. Sazak, C. J. Nelson, and B. Obara, "The multiscale bowler-hat transform for blood vessel enhancement in retinal images", *Pattern Recognit*., Vol. 88, pp. 739–750, 2019.

[21] M. A. U. Khan, J. N. Carmichael, A. Sarirete, and N. Mir, "Thin Vessel Detection and Thick Vessel Edge Enhancement to Boost Performance of Retinal Vessel Extraction Methods", *Procedia Comput. Sci*., Vol. 163, pp. 618–638, 2019.

[22] Z. Yan, X. Yang, and K. Cheng, "A Three-Stage Deep Learning Model for accurate retinal vessel segmentation", I*EEE J. Biomed. Heal. INFORMATICS*., Vol. 23, pp. 1427–1436, 2019.

[23] J. Dash and N. Bhoi, "A thresholding based technique to extract retinal blood vessels from fundus images", *Futur. Comput. Informatics J.*, Vol. 2 pp. 103–109, 2017.

[24] J. Dash and N. Bhoi, "An Unsupervised Approach for Extraction of Blood Vessels from Fundus Images", J. Digit. *Imaging.*, Vol. 31, pp. 857–868, 2018.

[25] A. Desiani, B. Erwin, S. Bambang, W. Yogi, C. E. Setyo, and M. Arhami, "VU-Net: A U-Net Modification by VGG-Batch Normalization for Retinal Blood Vessel Segmentation", *International Journal of Intelligent Engineering and Systems*, Vol. 15, No. 6, pp. 303-314, 2022, doi: 10.22266/ijies2022.1231.29.

[26] T. J. Jebaseeli, C. A. D. Durai, and J. D. Peter, "Segmentation of retinal blood vessels from ophthalmologic Diabetic Retinopathy images", *Comput., Electr., Eng*., Vol. 73, pp. 245–258, 2019.

[27] X. Wang, X. Jiang, and J. Ren, "Blood vessel segmentation from fundus image by a cascade classification framework", *Pattern Recognit*., Vol. 88, pp. 331–341, 2019.

[28] H. A. Ramos, J. G. A. Cervantes, I. C. Aceves, J. R. Pinales, and S. Ledesma, "Blood vessel segmentation in retinal fundus images using Gabor filters, fractional derivatives, and Expectation Maximization", *Appl., Math., Comput*., Vol. 339, pp. 568–587, 2019.

[29] D. U. N. Qomariah, H. Tjandrasa, and C. Fatichah, "Segmentation of Microaneurysms for Early Detection of Diabetic Retinopathy Using MResUNet", *International Journal of Intelligent Engineering and Systems*, Vol. 14, No. 3, pp. 359-373, 2021, doi: 10.22266/ijies2021.0630.30.

[30] L. C. Rodrigues and M. Marengoni, "Segmentation of optic disc and blood vessels in retinal images using wavelets, mathematical morphology and Hessian-based multi-scale filtering", *Biomed. Signal Process. Control*., Vol. 36, pp. 39–49, 2017.

[31] E. Cuevas, A. Rodríguez, A. A. Reyes, and C. D. V. Soto, "Blood Vessel Segmentation Using Differential Evolution Algorithm", *Recent Metaheuristic Comput. Schemes Eng.*, Vol. 948, pp. 151–167, 2021.

[32] M. A. U. Khan, F. Abdullah, A. Akram, R. A. Naqvi, M. Mehmood, D. Hussain, and T. A. Soomro, "A Scale Normalized Generalized LoG Detector Approach for Retinal Vessel Segmentation", *IEEE Access*, Vol. 9, pp. 44442–44452, 2021.

[33] G. R. Vidhya and H. Ramesh, "Effectiveness of contrast limited adaptive histogram equalization technique on multispectral satellite imagery", In: *Proc. Int. Conf. Video Image Process*., Roorkee, India, pp. 234-239, Dec. 2017.

[34] S. Roychowdhury, D. D. Koozekanani, and K. K. Parhi, "Blood Vessel Segmentation of Fundus Images by Major Vessel Extraction and Sub image Classification", *IEEE Journal of Biomedical and Health Informatics*, Vol. 19, No. 3, pp. 1118-1128, May 2015.

[35] A. Mendonca and A. Campilho, "Segmentation of retinal blood vessels by combining the detection of centerlines and morphological reconstruction", *IEEE Transactions on Medical Imaging*, Vol. 25, No. 9, pp. 1200–1213, 2006.

[36] M. Fraz, P. Remagnino, A. Hoppe, B. Uyyanonvara, A. Rudnicka, C. Owen, and S. Barman, "An ensemble classification-based approach applied to retinal blood vessel segmentation", *IEEE Transactions on Biomedical Engineering*, Vol. 59, No. 9, pp. 2538–2548, 2012.

[37] M. M. Fraz, S. A. Barman, P. Remagnino, A. Hoppe, A. Basit, B. Uyyanonvara, A. R. Rudnicka, and C. G. Owen, "An approach to localize the retinal blood vessels using bit planes and centerline detection", *Comput. Methods Programs Biomed*. Vol. 108, No. 600–616, 2012.

[38] Rashmi, M. Kumar, and R. Saxena, "algorithm and technique on various edge detection: a survey", *Signal & Image Processing, An International Journal (SIPIJ)*, Vol. 4, No. 3, June 2013.

[39] A. Hoover, V. Kouznetsova, and M. Goldbaum, "Locating blood vessels in retinal images by piecewise threshold probing of a matched filter response", *IEEE Transactions on Medical Imaging*, Vol. 19, pp. 203–210, 2000.

[40] K. U. Research, "Chase db1", January 2011, [Online]. Available: http://blogs.kingston.ac.uk/retinal/chasedb1/

[41] B. Toptas and D. Hanbay, "Retinal blood vessel segmentation using pixel-based feature vector", *Biomedical Signal Processing and Control*, Vol. 70, pp. 103053-103065, 2021.